Curve fitting of mixed-mode isopachics

R.I. Hebb, J. M. Dulieu-Barton, K. Worden[+], P. Tatum*

University of Southampton, School of Engineering Sciences, Highfield, Southampton, SO17 1BJ, UK

[+] Department of Mechanical Engineering, University of Sheffield, Mappin Street, Sheffield, S1 3JD, UK

[*]AWE, Aldermaston, Reading, Berkshire, RG7 4PR, UK

Abstract

Recent work has focused on exploiting the observation that the stress-sum contours (isopachics), obtained from TSA, in the vicinity of the tip take the form of a simple curve – the cardioid. The analysis made use of the cardioid nature of the isopachics by deriving expressions for the SIFs in terms of the cardioid area and the positions of certain tangents to the curve. Both Genetic Algorithms (GAs) and Differential Evolution (DE) have also proved successful for parameter estimation, but some of the curve-fits indicated that the cardioid form was inappropriate for the base model, particularly for mixed-mode cracks. The effect of crack-tip interaction has been explored and shows this has a small effect on the cardioid form. New, higher resolution infra-red detectors have become available since the original data was collected, so the object of the current paper is to use new techniques to extract the cardioid form and use a GA to perform the curve fitting.

1. Introduction

Thermoelastic Stress Analysis (TSA) is one of a group of full-field techniques for experimental stress analysis that has proved to be extremely effective for studying stress fields in the vicinity of crack-tips. An understanding of such fields is vital to the development of effective diagnosis and prognosis algorithms for Non-Destructive Testing (NDT) and Structural Health Monitoring (SHM). A means of undertaking crack-tip studies using TSA is based on the observation that the stress-sum contours (isopachics) in the vicinity of the tip take the form of a simple curve – the cardioid. This treatment is based on the first order Westergaard equations [1], or equivalently, the singular terms in the eigenfunction expansion of Williams [2], and was demonstrated in [3] where the Stress Intensity Factors (SIFs) were obtained for simulated cracks (in the form of spark eroded slots) in mode I and mixed mode opening. The analysis in [3] made use of the cardioid geometry of the isopachics by deriving expressions for the SIFs in terms of the cardioid area and the positions of certain tangents to the curve. This treatment was fully exploited in [4] by developing algorithms and software that automatically obtained the SIFs from the thermoelastic data and demonstrated that the technique could be applied to actual cracks. Other researchers have developed successful techniques for crack-tip stress studies, e.g. [5, 6] based on the Mushkelishvili stress function.

Recent work [7] has allowed the estimations of crack-tip SIFs by direct curve-fitting of the cardioid form to measured isopachics from TSA. One advantage of this approach is that the curve-fit also provides an accurate estimate of the crack-tip location. Both Genetic Algorithms (GAs) [7] and Differential Evolution (DE) [8] proved successful for the actual parameter estimation, but some of the curve-fits indicated that the cardioid form was inappropriate for the base model. One of the possible explanations for this is that the cardioid form is theoretically only suitable for an *isolated* crack-tip stress field, as derived from the Westergaard equations. In the experimental data for the previous studies, a crack was placed centrally in a plate and there will therefore have been two (potentially) interacting crack-tips involved (note that the term *interaction* is used rather loosely here, it simply means that the observed field is a linear superposition of fields from two crack-tips).

The object of this current paper is to demonstrate that the techniques developed for extracting the isopachics from the thermoelastic data in [7] can be applied to data obtained from high resolution infra-red systems. Since the data used in [7] was collected, higher resolution systems have become available which present new challenges in data extraction. Furthermore, the algorithm developed in [7] was targeted at using a selected number of isopachics. In this work the possibility of using the entire captured data set is explored. To do this, data has been collected using a high resolution device and a new approach to data extraction developed, which is described in the paper. The paper describes the progress made in applying the new approach by obtaining the curve-fitted isopachics.

2. Theory

Thermoelastic stress analysis is based on the measurement of small temperature changes that occur in solids on the application of a cyclic stress. It can be shown that the temperature changes are proportional to the changes in the sum of principal stresses [9]. The temperature changes are measured using a highly sensitive infra-red detector. By applying an appropriate calibration factor A, the detector output, S, known as the thermoelastic signal, provides a measurement of the stress-sum via:

$$AS = \Delta(\sigma_1 + \sigma_2) \tag{1}$$

There are various assumptions underlying this assertion: these are outlined in [9], where a review of the applications of TSA is presented. In order to extract information relating to SIFs, appeal is made to the Westergaard equations [1], and it can be shown that in the vicinity of the crack-tip (but not the immediate vicinity where plasticity is a factor and Linear Elastic Fracture Mechanics (LEFM) does not apply) the stress sum is related to the mode 1 and mode 2 SIFs K_I and K_{II} by:

$$\Delta(\sigma_1 + \sigma_2) = \Delta(\sigma_x + \sigma_y) = \frac{2K_I}{\sqrt{2\pi r}}\cos\left(\frac{\theta}{2}\right) - \frac{2K_{II}}{\sqrt{2\pi r}}\sin\left(\frac{\theta}{2}\right) \tag{2}$$

where r and θ are polar coordinates centred at the crack-tip with θ measured anti-clockwise from the crack-line. An elementary rearrangement of this formula yields:

$$r = \frac{K_I^2 + K_{II}^2}{\pi A^2 S^2}\left[1 + \cos(\theta + 2\phi)\right] = \frac{r_0}{2}\left[1 + \cos(\theta + 2\phi)\right] \tag{3}$$

where $\phi = \tan^{-1}(K_{II}/K_I)$ is the rotation of the cardioid and r_0 is the maximum radial coordinate of the cardioid curve. Equation (3) shows that a curve of constant signal, S, is a cardioid. The method used in [4] to determine the SIFs was to carry out a nonlinear least-squares curve-fit of equation (3) to constant S contours extracted from the thermoelastic images, and thus determine r_0 and φ for given S. Given this data, the SIFs are computed by solving the following simultaneous equations:

$$K_I^2 + K_{II}^2 = \pi r_c A^2 S^2 \quad \text{and} \quad \tan\phi = \frac{K_{II}}{K_I} \tag{4}$$

In the current work it is proposed to used the GA approach described in [7].

3. TSA System

Infra-red imaging equipment is constantly being improved as the underlying technology quickly advances. The system used to collect the data described in this paper is the Silver 480M system manufactured by Cedip Infrared Systems. The detector elements in the camera are made from indium antimonide with an array size of 320 x 256. Two arrays are present in the detector, with one array over-layed on top of the other. Each array has its own internal buffer used for data storage. This set-up allows the arrays to be used sequentially, with one array collecting the incoming photons, and the other transferring data to its internal buffer. Consequently, a faster frame rate and a more continuous data capture process than using a single array is possible (e.g. the Deltatherm system [9]). The maximum frame rate of the entire system (with processing) is 383Hz, although a faster frame rate can be achieved using windowing. Windowing operates by only sending data from a certain region on the array, thus processing time is reduced as less data is supplied. For the processing, a dedicated processor housed within the camera itself digitizes the voltage from each detector element, before sending it to the computer as a digital signal with units of `digital level' (DL) or S as given in equation (1). The data are output in a Comité Consultatif International des Radiocommunications (CCIR) phase-alternate line (PAL) video format, and sent to a Cedip FG9800 frame grabber card in the computer.

The Silver system has been radiometrically calibrated, so the temperature in an image can be automatically obtained from the DL data output by the detector. To do this four calibration files have been supplied by the manufacturer for four separate temperature ranges within an overall temperature range of 5 to 200°C. To calibrate the ΔDL data to ΔT, the mean temperature of the specimen is measured at each pixel, and the gradient of the calibration curve for that temperature is used to calculate the ΔT value [10].

4. Test Specimens and set-up

The dimensions of the plate specimen considered here is shown in Figure 1. The plate was manufactured from Duralumin® and has dimensions 300 x 300 mm with a thickness of 1.7 mm. At the centre of the plate a small hole has been drilled and a spark eroded slot of total length 50 mm has been produced from the central hole. The 'crack angle', β, (see Figure 1) is 45°. To spread the load as evenly as possible across the width of the plate when mounted, 15 holes (at both the top and bottom of the plate) of 6 mm diameter so that the load is imparted into the plate through pins fixed in the holes. Bonded to the front and back at the top and bottom are 4 Duralumin® tabs 6 mm thick and 30 mm wide. The purpose of these tabs is to locally strengthen the area around the holes. The specimen was mounted in an Instron 8800 servo-hydraulic machine using jigs that comprised 4 sheets of steel 12 mm thick. Two sheets are bolted either side both top and bottom of the specimen. Each sheet has a 16 mm hole through which connecting pins are slotted, so that another 12 mm steel tab can be connected to the plates. This tab is then gripped by the jaws of the machine. Figure 2 shows the specimen with the top mounts connected (only the top mounts have been shown for clarity).

Before experiments can be performed, the surface of the specimen being viewed by the infra-red detector needs to be treated. Previous work has shown that it is extremely difficult to obtain workable results from a plain untreated metallic surface [11], because of reflected radiation and variations in the surface. To prepare the surface, it is firstly cleaned with acetone and dried. If required, the surface can also be polished to obtain the smoothest surface possible. Once clean and smooth, two thin layers of

matt black paint are applied (with the first layer being allowed to dry before application of the second). The specimen was mounted centrally in the servo-hydraulic test machine, and the infra-red detector was positioned to examine the crack-tip. The frequency and amplitude of the cyclic loading was controlled by the test machine.
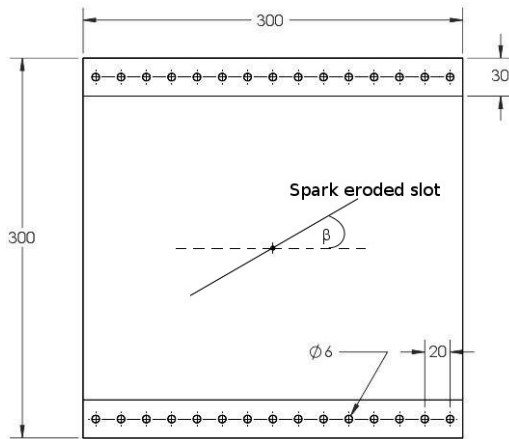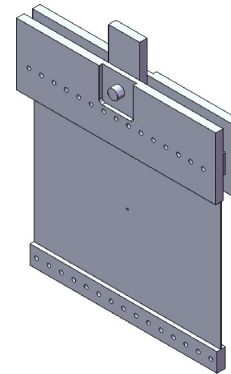

Figure 1: Specimens tested   Figure 2: Loading jig

5. Extracting Isopachics from the Thermoelastic Data

The GA fits a curve to the coordinates of the isopachics, which are input as a list of (x, y) values. To extract these values the thermoelastic data is first loaded into Altair (software supplied with the Cedip system). Altair has an 'area' function, where a rectangular area can be selected in the data, and various forms of information obtained from that area. One function is to copy the the thermoelastic data from each pixel to an external text file. Therefore, by choosing an area around the region of interest, the values of relevant pixels can be obtained. The number of desired results (N) is input to the program at this stage (this decides how many 'sets' of values to create). The header of the copied text file contains the minimum and maximum values present in the area selected. The program uses the minimum and maximum values to calculate the range of values present in the list and then divides this range into N equally spaced bins, creating a blank text file for each bin.

a) Full field data   b) Example of an   c) Complete curve with data   d) Complete data set
                             incomplete curve   extending beyond the array   contained within the array
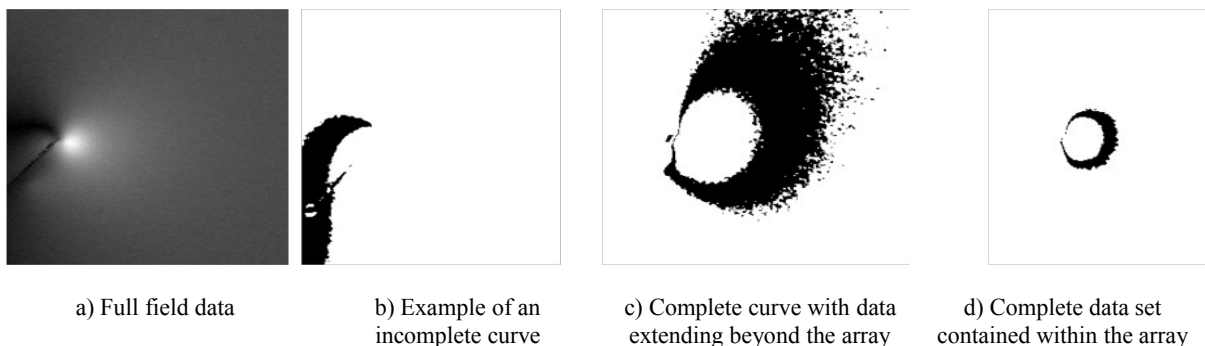
Figure 3: Processing the thermoelastic data to input into GA

Moving through the list, the program compares the value of each (x, y) coordinate to the bins, and appends the x and y values to the relevant bin's text file. An example of the process can be seen in Figure 3 where (a) is the thermoelastic data used and the other three images are three of the bins

produced. Image (b) is an example of an incomplete curve in the data sets. The data points for this set continue through the bottom left corner and to the other tip of the slot. Similarly, (c) is an example of a data set where the range continues outside of the image boundary. Cases like (b) and (c) are not used for curve-fitting process. Image (d) is an example of a complete closed curve which would be suitable for analysis. However, the GA requires coordinates of a single curve, as opposed to a range of curves. Therefore, the coordinates of a line that would bisect each area of pixels is required. If the data points lay on a horizontal line as opposed to a closed curve, then all that would be required is a simple averaging procedure over the length of the line.

When the polar coordinates of a circle (with its centre on the origin) are plotted as r against θ the end result is a constant. The same process is performed on the data sets by transforming the coordinates of the pixel locations from Cartesian to the polar coordinate system. In Altair, a point near to the crack tip is chosen (as this will be near the centre point of each closed curve) and this point is defined in the program to be the origin of the polar coordinate system. The program then loads each data set in turn. Running through the currently loaded data set, the (x, y) positions of the data are transformed to polar coordinates and put into a new array which is ranked according to increasing θ. The number of points (P) required in the final curve is decided (e.g. 100). Using the newly created array, the full range of θ is divided into P bins, with the mean r of the points contained being calculated for each bin. Each bin is therefore assigned a θ and r coordinate. Once all P bins have been averaged, the polar coordinates of the bins are transformed back into Cartesian coordinates. Here the origin is defined as the bottom left corner of the original image, as previously the origin was the top left which is the standard method in images. Figure 4 illustrates the process. Firstly a dataset is loaded as shown in Figure 4a. All of the points are transformed to polar coordinates and the mean r is then calculated for each bin (the over layed blue points)- see Figure 4b. Both sets of mean r and the original data are then converted back to the Cartesian coordinate system (Figure 4c), with the image in Figure 4d showing the resulting isopachic. It is these coordinates that are used in the GA for the curve-fitting process.
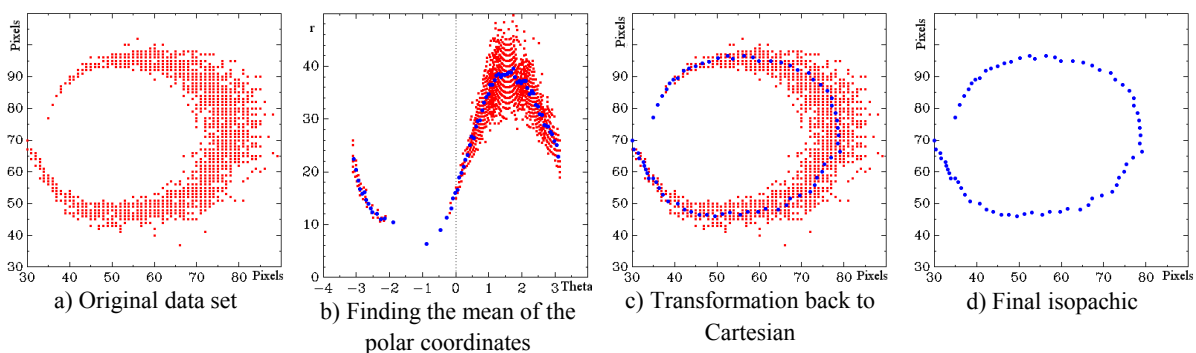

a) Original data set   b) Finding the mean of the polar coordinates   c) Transformation back to Cartesian   d) Final isopachic

Figure 4: Demonstration of the averaging technique to reduce a data set to a single isopachic

6. Results

Figure 3(a) is from the plate with β = 45°. The applied stress range is 9.81 MPa with a loading frequency of 10 Hz. This view differs to the actual data obtained only in the fact that it is a crop of the full field. The data was analysed to produce 20 isopachics, and Figure 5 shows the odd numbered isopachics that result from the averaging process (only the odd numbered curves have been shown for clarity). One immediately striking observation is that not all of the isopachics take the cardioid form. Curves 1 and 2 are explained by the fact that the regions of constant S that they represent do not make a complete curve, with an example being Figure 3(b). Curve 3 has squared edges because the region of constant S is larger than the selected area in the original image. Data sets of this kind (either incomplete curves or having values outside of the boundary) are not used in the GA. It can also be noticed that the curves also provide negative y values. The original data doesn't have any negative y-

values for positions, as image coordinates start at (0, 0) and are always positive. This is an issue that needs to be rectified.
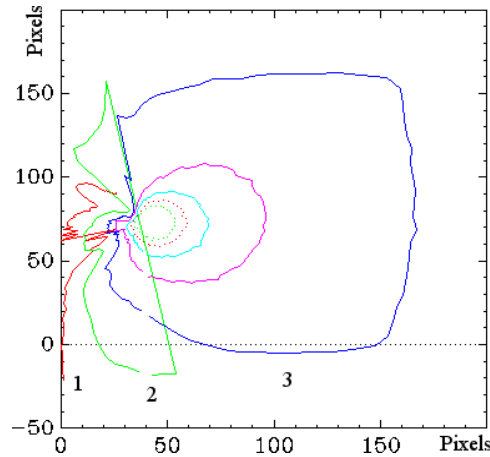

Figure 5: Odd numbered isopachics for the data shown in 4a

Results of running the GA using the isopachics from Figure 5 are provided in Figure 6. Here the isopachics have been extracted (circular data points) and the GA performed curve fitting to them. Table 1 shows the results of the GA for each data set (position of the cusp in terms of pixels, r_0, rotation angle and fitness) with the cardioid numbers set for 1 being the largest cardioid and 5 the smallest. The fitness parameter provides a means of comparing the suitability of each individual to the rest of the population by assigning a single number to each individual. Individuals are selected for mating based on their fitness so the fitter an individual is then the more likely it is to be selected for the mating process to provide better solutions in subsequent generations. The fitness function used is based on a mean-square error (MSE) for the curve fit. If the measured points on the cardioid are denoted by (r_i, θ_i), $i = 1, \ldots, N$, the MSE is defined by:

$$M = \frac{100}{N\sigma_r^2} \sum_{i=1}^{N} \left(r_i - r_{ie}\right)^2 \qquad (5)$$

where r_{ie} is the estimate from the curve-fit and σ_r^2 is the variance of the array of measured radii. The fitness is the reciprocal of the normalised MSE, with the normalization of the MSE chosen so that a value of less than 5 for the MSE indicates a good fit to the data, and less than 1 being an excellent fit.

The actual location of the slot tip can be obtained examining the thermal image of the specimen, and it occurs at (34, 77) pixels; the estimated error on this value is around $\pm$ 2 pixels. For the (x, y) position of the cusp, all of the generated cardioids have their x-position shifted to the right of the slot-tip by as much as 10 pixels which equates to 3 mm. Figure 7 shows a zoomed region around the slot tip. Arrow A points to the actual location of the slot-tip, and arrow B points to (41, 80), which is the mean of the generated cusps' coordinates. An inspection of Figure 6 shows that the GA fits much better curves to the smaller isopachics than the larger curves. This may be explained by the fact that the Westergaard equation is only fully valid for situations where $r << a$ [1], so as the size of the isopachic increases, so the accuracy in the generated solution decreases. Cardioid 1 had a maximum radial distance from the cusp of 26.7 mm i.e. > than the 25 mm slot length and its cusp is located furthest away from actual slot-tip location and from the other slot-tips. Neglecting this data improves matters giving the average location of the slot-tip at (40, 78) shown by arrow C in Figure 7. Using the three smallest cardioids provides a relative position of the slot tip to within less than 1 mm, which is comparable to that achieved in previous work [7, 8]. The actual average position of the slot is (10.2, 23.1) mm and it can

be seen that the y location has been located precisely although the x location disagrees by about 2 mm. This warrants further investigation but is encouraging.

Table 1: Results of the GA fitting curves to isopachics

Cardioid Number	x (pixels (mm))	y (pixels (mm))	r_0 (pixels (mm))	2φ (radians)	Fitness
1	45.75 (13.7)	89.30 (26.8)	89.02 (26.7)	0.289	0.35978
2	41.99 (12.6)	80.79 (24.2)	53.86 (16.2)	0.393	0.49101
3	40.23 (12.1)	76.82 (23.0)	37.98 (11.4)	0.338	0.61657
4	39.41 (11.8)	77.39 (23.2)	29.48 (8.8)	0.442	0.58084
5	39.30 (11.8)	77.11(23.1)	23.82 (7.1)	0.497	0.55064

It can also be noted that the cardioids tend to rotate more as they approach the slot tip. This rotation is a current area of study, as the GA works on an idealised cardioid as the base model, which may not be technically correct. The cause of the rotations is currently not fully understood so at this stage the SIFs for these results have not been calculated.
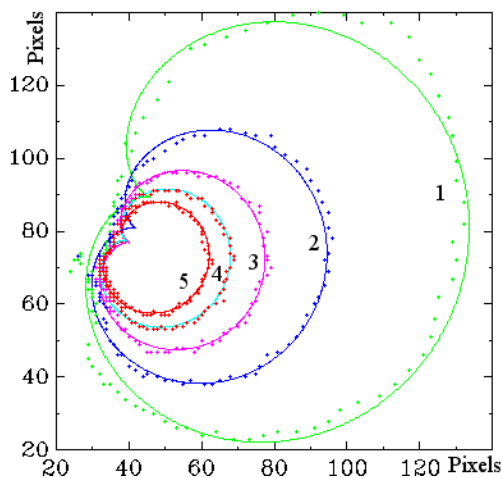

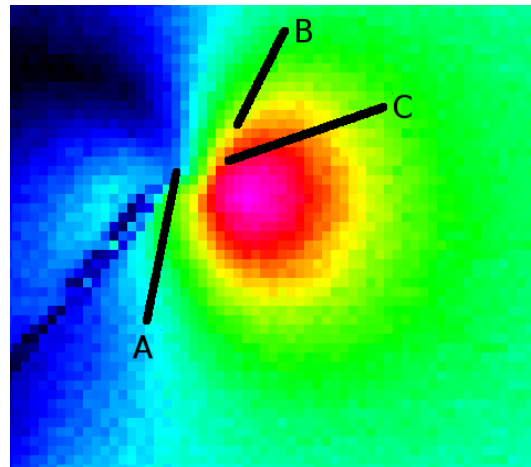Figure 6: Curve fitting to the isopachics (units in pixels)

Figure 7: Actual slot tip location (A) compared to the location calculated by the GA (B). Arrow C shows the location when cardioid 1 is neglected.

7. Conclusions and Future Work

The work in this paper has demonstrated that it is possible to use the existing GA routine for curve-fitting isopachics using data from the whole field. An approach has been developed for extracting data from the supplier's software that can be input into the GA algorithm. The approach has been demonstrated on a 45° slot. The results are encouraging in that the estimation of the position of the slot-tip is good using cardioids close to the slot tip. However, the cardioids are not 'nested' but are rotated. It is considered that this inaccuracy centres on the use of the first order Williams stress function and that an improved fit can be obtained using the full Williams stress function:

$$ AS = \frac{2\sqrt{|K_I^2 + K_{II}^2|}}{\sqrt{2\pi r}} \cos\left(\frac{\theta}{2} + \phi\right) + T_S + 2\sqrt{A_I{}^2 + A_{II}{}^2}\,\sqrt{r}\,\cos\left(\frac{\theta}{2} - \tan^{-1}\frac{A_{II}}{A_I}\right) + O\left(\sqrt{r}\right) \qquad (5) $$

where A_I and A_{II} are geometry-dependent constants.

Using the GA on thermoelastic data obtained for various r and β will enable an understanding of the cause of the cardioid rotations observed in the data.

It is also considered that the use of a slot instead of an actual crack is not desirable therefore in future work new specimens will be manufactured that contain mixed mode cracks. The method to obtain plates will involve spark eroding a horizontal slot in larger plate and then subjecting it to a fatigue load until the desired crack length is grown. Then a smaller plate will be cut out to give the necessary crack angle.

References

1　Ewalds, H L and Wanhill, R J. *Fracture Mechanics*. Arnold, London, 1991.

2　Williams, M L. On the stress distribution at the base of a stationary crack. *Journal Applied Mechanics*, 24 (1957).

3　Dulieu-Smith, J M and Stanley, P. Progress in the thermoelastic evaluation of mixed-mode stress intensity factors. In *Proc. SEM Spring Conf. on Expt. Mech.* (Dearborn 1993), 617-629.

4　Dulieu-Barton, J M, Fulton, M C, and Stanley, P. The analysis of thermoelastic isopachic data from crack tip stress fields. *Fatigue Fract. Engng. Mater. Struct.*, 23 (1999), 301-313.

5　Tomlinson, R A, Nurse, A D, and Patterson, A. On determining the stress intensity factors for mixed mode cracks from thermoelastic data. *Fatigue Fract. Engng. Mater. Struct.*, 20, 2 (1997), 217-226.

6　Tomlinson, R A and Marsavina, L. Thermoelastic investigations for fatigue life assessment. *Exp. Mech.*, 44 (2004), 487-494.

7　Dulieu-Barton, J M and Worden, K. Genetic identification of crack-tip parameters using thermoelastic isopachics. *Meas. Sci. Technol.*, 14 (2002), 176-183.

8　Dulieu-Barton, J M and Worden, K. Identification of crack-tip parameters using thermoelastic isopachics and differential evolution. *Key Engineering Materials*, 245-246 (2003), 77-86.

9　Dulieu-Barton, J M and Stanley, P. Development and applications of thermoelastic stress analysis. *Journal of Strain Analysis for Engineering Design*, 33 (1998), 93-104.

10 Fruehmann, R K, Dulieu-Barton, J M, and Quinn, S. On the thermoelastic response of woven composite materials. *Journal of Strain Analysis for Engineering Design*, 43 (2007), 435-450.

11 Dulieu-Barton, J M and Quinn, S. Identification of the sources of non-adiabatic behaviour for practical thermoelastic stress analysis. *Journal of Strain Analysis for Engineering Design*, 37, 1 (2002), 59-71.